

C – CORE TOPOLOGY FOR PM WIND GENERATORS WITH NON-OVERLAP IRON-CORED STATOR WINDINGS

*J.H. van Wijk**, *M.J. Kamper*[†]

*Department of Electrical and Electronic Engineering,
Stellenbosch University, Private Bag X1, 7602, Matieland, South Africa
14205009@sun.ac.za †kamper@sun.ac.za

Keywords: PM, wind generator, non-overlap windings.

Abstract

This paper presents the study of a C-core topology for direct-drive PM synchronous wind generators (PMSGs) with non-overlap iron-cored stator windings. Some of the most common challenges regarding wind energy converters are first considered, leading to the development of the C-core topology concept and the theory behind it. Results from the finite element (FE) simulations are presented and finally the C-core topology is implemented into a conceptual PMSG and compared, on a 300 kW power level, to a PM conventional synchronous generator manufactured locally.

1 Introduction and problem statement

Environmental awareness has stimulated the use of renewable energy regardless of the cost disadvantages that it poses. For wind energy converters these disadvantages are greatly influenced by the efficiency of the power transmission system and the generator [1],[2].

The three most common generator systems used to exploit wind energy today are the constant speed wind turbine with squirrel cage induction generator, the variable speed wind turbine with doubly-fed induction generator and the variable speed wind turbine with direct-drive synchronous generator [1].

Induction generators require a mechanical gear unit in the transmission to step up the rotational speed of the turbine to the desired generator operating speed. The continuous increase in rated power of wind turbines has led to unfavourable transmission ratios and the use of gearboxes rated at double the operating torque just to withstand the high rotor torque fluctuations caused by the pulsating nature of wind energy [2]. When efficiency and mass are considered, gearboxes are regarded unfavourable [3]. Gear unit losses, component wear, maintenance, and noise emission are further disadvantages of conventional mechanical transmissions.

Synchronous generators can operate at very low speeds and therefore a direct-drive synchronous generator system does not need a heavy gearbox between the turbine and generator.

However, in order to produce the specified power output, direct-drive synchronous generators require large bore diameters in order to produce high torque. Compared to standard conventional induction generators, direct-drive synchronous generators are more expensive [1]. Their large diameters make them much larger and heavier than induction generators.

Most direct-drive synchronous generators are electrically excited, but permanent magnet synchronous generators (PMSG) are ideal for direct-drive applications because of their high force density and high efficiency [4],[5]. Using PM excitation reduces the rotor material volume and eliminates all excitation losses in the rotor.

Because the magnetic excitation cannot be controlled when using PMs, the attraction forces between rotor and stator iron parts, pose challenges during generator assembly and tend to dominate the structural design [6]. Bulky structural construction is often required in order to prevent air gap closing after assembly and during operation. Bulky construction is one of the largest contributors to the mass and cost of synchronous generators.

In this study the attraction forces between the rotor and stator iron part are addressed and the aim of the topology introduced in this paper is to eliminate leakage flux. The goal in this study is also to reduce the structural material, and hence mass, using the presented rotor yoke topology.

2 Theoretical Concept Development

In order to address the strong attraction forces between the rotor and the iron-cored stator a basic understanding of electromechanical-energy conversion principles is of essence. Figure 1 shows the general path of magnetic flux in a conventional PMSG. Figure 2 is a simplified schematic of the electromagnetic circuit, portraying a pole pitch section of such a conventional PMSG, where the stator slots and teeth are neglected.

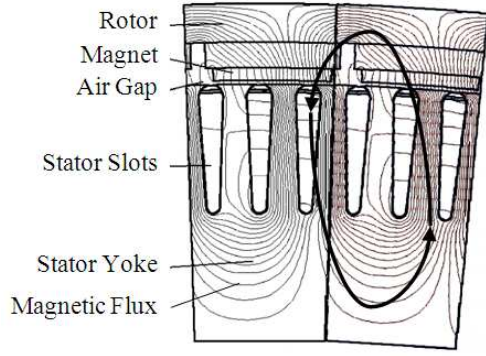


Figure 1: Magnetic flux path in conventional PMSG.

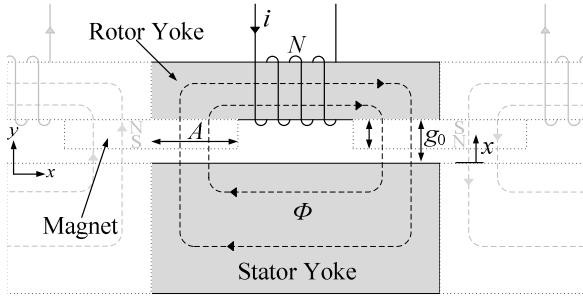


Figure 2: Magnetic flux schematic: conventional PMSG.

The following assumptions regarding the electromagnetic circuits are made to simplify analysis:

- Lossless system
- No flux leakages around magnet sides
- No flux fringing
- Linear magnetic system

The stored co-energy, W'_{fld} in the field (or air gap, g) is a state function, where i and x are its two independent state variables. The field attraction force, f_{fld} produced by the magnetic field is defined as the partial derivative of the magnetic stored co-energy in the air gap, g with respect to a displacement, x , while keeping the excitation current, i constant. This is written as

$$f_{fld} = \left. \frac{\partial W'_{fld}(i,x)}{\partial x} \right|_i \quad (1)$$

Because of the dominant air gap, the system is assumed linear ($\lambda=Li$) [7]. The stored co-energy in the air gap is therefore defined as

$$W'_{fld} = \frac{1}{2}L(x)i^2 \quad (2)$$

The circuit inductance, L is a function of the reluctance of the magnetic flux path, Φ and hence inherently dependent on the effective air gap length, $g(x) = (g_0 - x)$. The expression for inductance is

$$L(x) = \frac{N^2}{\mathcal{R}(x)} = \frac{\mu_0 AN^2}{g(x)} \quad (3)$$

From Equation (1) - (3) the field attraction force, f_{fld} is

$$f_{fld} = \frac{\mu_0 AN^2 i^2}{2} \frac{\partial}{\partial x} \left(\frac{1}{g(x)} \right) \quad (4)$$

The schematic in Figure 2 shows the total effective air gap, $g(x)$ for the flux path to be

$$g(x) = 2(g_0 - x) \quad (5)$$

The constant, g_0 is the design air gap length. Substituting Equation (5) into Equation (4) and differentiating, gives

$$f_{fld} = \frac{\mu_0 AN^2 i^2}{4(g_0 - x)^2} \quad (6)$$

Equation (6) can be rewritten to give the following well known expression for the force on the stator in terms of flux density, B

$$f_{fld} = \frac{B^2 A}{\mu_0} \quad (7)$$

It is clear that the force produced by the magnetic field is inversely proportional to the square of the effective air gap length of the generator.

For conventional generators any closing of the air gap results in an opening at the opposite side of the generator and therefore a force imbalance on the stator and rotor is created. Even if the air gap is equal everywhere in the generator, Equation (7) shows that the presence of any flux density in the air gap of conventional generators produces attraction forces between its stator and rotor. For this reason bulky mechanical structure is required to ensure sufficient stiffness.

Figure 3 illustrates a simple schematic of the magnetic circuit of a PMGS with a double rotor topology. This topology introduces a second air gap. At each air gap leakage fluxes (Φ_1 and Φ_2) are present between the neighbouring magnets. The mutual flux, Φ_3 , has a constant reluctance ($g = 4g_0$), independent of the stator position, x , and therefore does not contribute to the magnetic field force experienced by the stator.

The effective air gap for flux path Φ_1 is given by Equation (5) and therefore the magnetic field force experienced in the air gap is also described by Equation (6). Flux path Φ_2 has an effective air gap length of

$$g(x) = 2(g_0 + x) \quad (8)$$

Substituting Equation (8) into Equation (4) and differentiating, gives a negative expression for the magnetic field force due to the second air gap.

$$f_{fld} = -\frac{N^2 i^2}{\mu_0 A \mathcal{R}^2(x)} = -\frac{\mu_0 AN^2 i^2}{4(g_0 + x)^2} \quad (9)$$

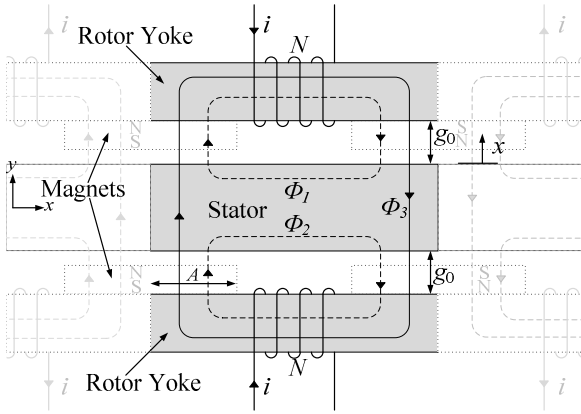


Figure 3: Magnetic flux schematic: double-rotor PMSGs.

From Equation (6) and (9) it can be seen that when the two air gap lengths are equal ($x = 0$), the resultant force on the stator is theoretically zero. Any shift of the stator will decrease the reluctance of the closing air gap, therefore resulting in an increase of the attraction force. The opposite is true for the opening air gap which experiences an increase in reluctance and therefore a drop in the field attraction force.

Figure 4 shows a schematic where the rotor yoke between the neighbouring magnets is removed. An alternative flux path between the magnet pairs is provided. The effective air gap length for flux path Φ_1 and Φ_2 is $2g_0$ and for Φ_3 is $4g_0$. The reluctance of the model stays unchanged for any stator position, x . The field force due to the air gap flux density, acts only on the two rotor yokes. It is expected that the force produced by the leakage flux, Φ_1 and Φ_2 , in Figure 3 will be eliminated.

This decoupling of the stator and its position from the magnetic field force, f_{fld} is what led to the development of the conceptual topology presented in this paper. The C shaped yoke provides the alternative path between the magnet pairs for the flux. Figure 5 presents the C-core topology in a conceptual 300 kW PMS wind generator.

The air gap between every neighbouring pole pair and yoke, as seen in Figure 6, acts as a barrier for the flux between adjacent yokes and hence theoretically eliminates the flux leakage paths between neighbouring magnets, as found in conventional and double rotor generators.

The pole pitch, p_p is governed by the inner diameter of the yoke arrangement, where they are closest to each other. Allowing for a spacing that is larger than $2g_0$ at the inner diameter, the maximum allowable ratio of magnet pitch, p_m to pole pitch is calculated to be 0.77, which is less than the 0.9 of the 300 kW conventional generator that was built. Although a lower pole pitch ratio reduces the volume of material, it also has a negative effect on the torque produced by the generator. In a performed study it was found that the extent of this drop in torque is not more than 5% when the ratio of magnet pitch to pole pitch is reduced from 0.9 to 0.71.

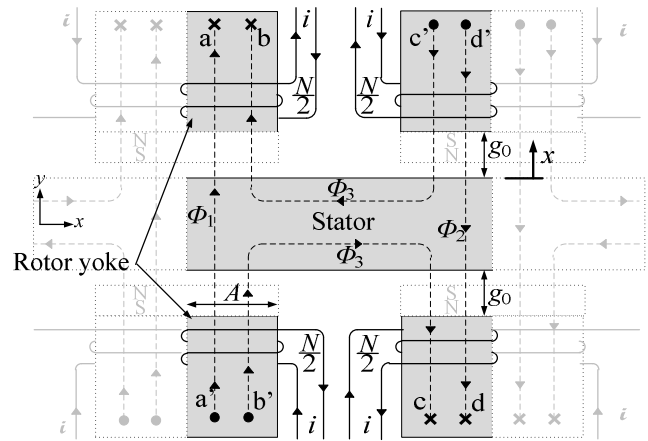


Figure 4: Magnetic flux schematic: C-core PMSG.

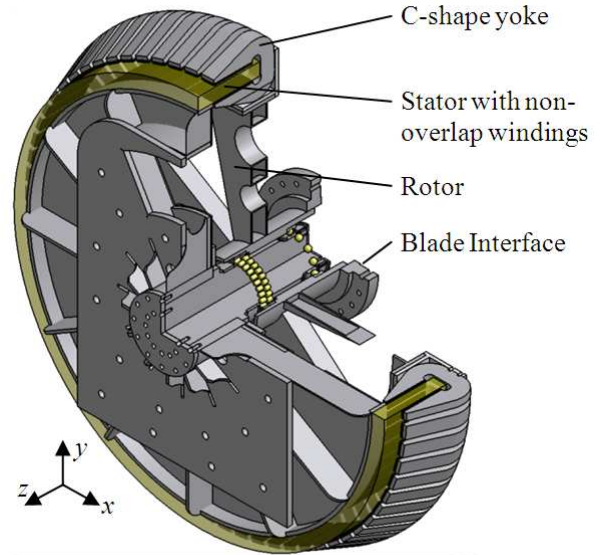


Figure 5: 300 kW C-core PMSG.

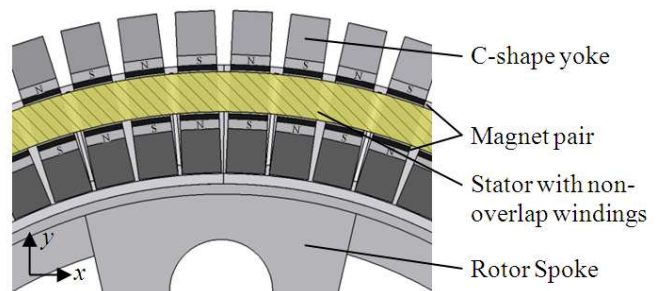


Figure 6: Head-on view of yoke placement.

3 Finite Element Analysis

3.1 Mechanical Analysis

Yoke dimensions and stator position influence the flux density, B_g , in the air gaps. In this study the maximum B_g in the closing air gap never exceeded 1.2 T. The maximum allowable air gap closing is taken to be 10% of g_0 . The yoke height, h_Y required of this condition is calculated to be 52 mm for the 300 kW generator of Figure 5. Magnetic FE simulations show that this yoke height causes the yoke to be deep in magnetic saturation, which has a limiting effect on the B_g . The yoke height is increased in steps until a favourable B_g is obtained.

A yoke height of 85 mm proves to satisfy the air gap flux density requirement. Deformation calculations, done on a cantilever with uniform cross section, show that the air gap closing reaches a maximum of 2.27%. Although the tapering ends of the yoke, seen in Figure 7, are not accounted for, FE strength analysis confirms this result by predicting an air gap closing of 2.95%. Figure 8 shows an exaggerated graphic FE result, representing the deformation of the C-core yoke. The weight of a single pole unit (including the magnet pair) is calculated to be 33.5 kg for the generator in Figure 5.

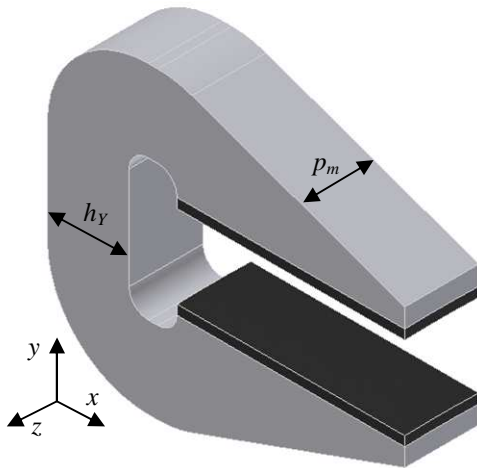


Figure 7: C-core yoke.

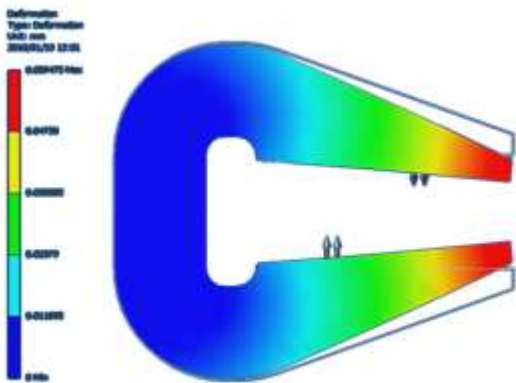


Figure 8: Pole strength analysis results.

Non-overlap stator windings prove to be a good choice for the stator winding configuration. The stator thickness has a uniform thickness which allows the stator to be easily inserted into the yoke arrangement from the front (z -direction). Non-overlap windings also allow the stator to be manufactured in modules/sections which has various advantages for assembly and maintenance purposes.

3.2 Magnetic Analysis

Magnetostatic FE analyses show that, contrary to what was expected, attraction forces between the rotor and iron-cored stator of the generator do exist when $x \neq 0$. These attraction forces can only be attributed to the presence of leakage flux in the model as described in the theory. The study shows further that the spacing between the individual yoke units has very little influence on the field force for a fixed stator position, $x > 0$. But secondly it is found that the attraction forces are attributed to the leakage flux located around the magnet-yoke interfaces.

To put the magnitude of these attraction forces into perspective, the forces are determined for three scenarios – first for the stator position $x = 0$, then for a 10% closing of the air gap ($x = 0.1g_0$) and finally an extreme case where the air gap closing is one fourth of g_0 ($x = 0.25g_0$). Table 1 shows the result of the study where these scenarios are applied to the three topologies discussed in Section 2. A 2-pole pitch section of each topology is modelled with a solid iron piece as the stator, as shown in Figure 10. The force on the stator for the conventional topology is found to be 12,9 kN and this value is taken as unity.

Topology	$x = 0$	$x = 0.1g_0$	$x = 0.25g_0$
Conventional	1	1.06	1.16
Double rotor	< 0.01	0.1	0.27
C-core	< 0.01	0.065	0.19

Table 1: Field force comparison with solid iron stator at three different stator positions.

From Table 1 it is noticeable that both the double rotor and the C-core topologies are very effective in reducing the large field forces found in conventional generators. It is expected that a solid iron stator will experience the greatest attraction forces compared to slotted stators at a specified stator position, x . For the C-core topology, the forces on two stator designs are compared to that of a solid iron stator and tabulated in Table 2. The effect that the slot iron rib thickness, t , as shown in Figure 9, has on the attraction field force is also investigated. Table 2 shows that the open slot stator design can further reduce the force on the stator by 75% -90%.

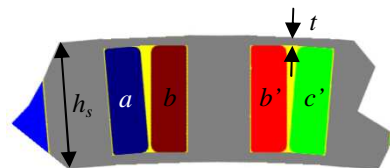


Figure 9: Closed slot stator design with rib thickness, t .

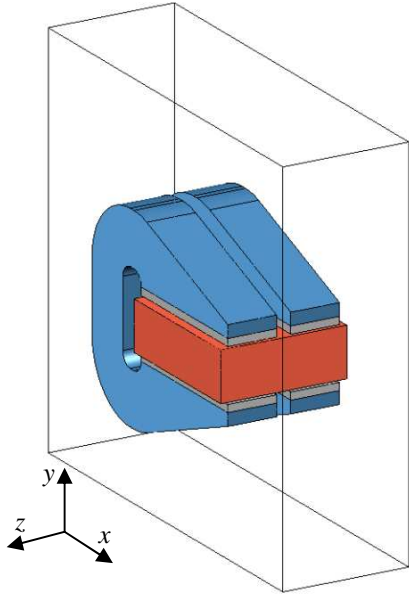


Figure 10: Magnetic FE model.

Stator configuration	unity force
Solid stator	0.19*
Closed slot – t = 2.5mm	0.1
Closed slot – t = 2 mm	0.08
Open slot – t = 0 mm	0.03

* value taken from Table 1 for the C-core topology.

Table 2: Stator design force results at $x = 0.25g_0$.

Depending on the stator construction, open slot stators have the advantage that coils can be pre-wound and easily inserted into the slots, where for semi-closed and closed slot designs, the coils need to be turned onto the stator teeth, a very laborious process.

4 Mass Comparison

The mass of the conceptual 300 kW PM synchronous wind generator, presented in Figure 5, is estimated to be 6884 kg. This is 15% heavier than the estimated 6035 kg of the 300 kW conventional PM synchronous generator. The mass contribution of the different generator components to each generator's own mass is presented in Figure 11 and Figure 12.

Figure 11 clearly shows that the stator and structural material contribute two thirds of the overall mass of the conventional PMSG. Figure 12 on the other hand shows a mass contribution of 44% for the same components, 8% reduction in structural mass and 15% reduction in stator material.

One drawback of the C-core topology is the remarkable contribution the rotor yoke makes to the total mass of the generator. This is easily seen from Figure 12. In order to make the generators more comparable, the total mass of the conventional generator is taken as unity. These results are tabulated in Table 3.

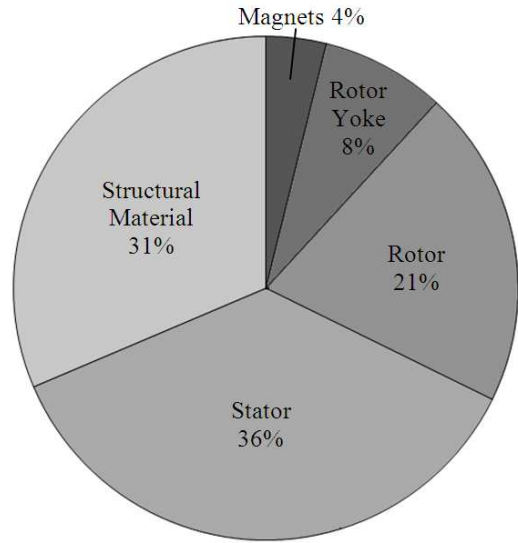


Figure 11: Mass distribution of components: Conventional 300 kW PMS wind generator.

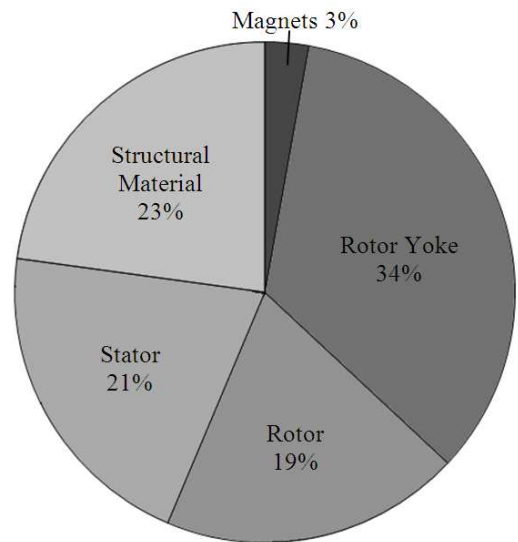


Figure 12: Mass distribution of components: Conceptual 300 kW C-core PMS wind generator.

Generator components	Conventional	C-core
Magnets	0.04	0.03*
Rotor yoke	0.08	0.39
Rotor	0.21	0.23
Stator	0.36	0.24
Structural materials	0.31	0.26
Total mass contribution	1	1.15

* The smaller magnet mass contribution is explained by the drop in the p_p to p_m ratio.

Table 3: PMSG per unit mass comparison.

5 Conclusion

From this study and the results presented in this paper, the following conclusions are drawn:

- PMs make generator assembly very difficult where large stator and rotor units are involved. The modular design of the C-core units, promise to make handling easier during the assembly process. The modular design also allows the individual core units to be adjusted individually to ensure uniform air gap throughout the generator. The stator can also be assembled from modular units if concentrated non-overlap windings are used.
- Attraction forces between rotor and stator iron parts of both the double rotor and the C-core PMSG show a dramatic reduction compared to the forces in conventional PMSGs. Interestingly the difference between the double rotor and the C-core PMSG is very little. This is explained by the leakage flux around the magnet ends that will always result in some degree of attraction force on the iron-cored stator. A further reduction of these forces is found when an open slot design is used.
- The C-core topology proved to reduce the structural and stator material mass of the conceptual design greatly. Unfortunately the total yoke mass counters this reduction in mass. Nevertheless, even though the overall mass is larger, compared to the conventional generator, it is not unrealistic. The conceptual design used is a first and not the optimum design.
- The yoke height and therefore also the yoke mass, are shown to be determined by the electromagnetic design of the pole core and not the mechanical strength criterion.

Acknowledgements

The financial assistance of the South African National Energy Research Institute towards this research is hereby acknowledged. Opinions expressed and conclusions arrived at, are those of the author and are not necessarily to be attributed to SANERI.

References

- [1] H. Polinder, S. W. H. De Haan, M. R. Dubois. "Basic Operation Principles and Electrical Conversion Systems of Wind Turbines", *EPE Journal*, **15**, pp. 43-50, (2005)
- [2] S. Jöckel. "Gearless Wind Energy Converters with Permanent Magnet Generators – An Option for the Future?", *Proc. European Union Wind Energy Conference*, 1996, pp. 422-428, Göteborg, Sweden, 20-24 May
- [3] N. Hodgins, A. McDonald, J. Shek, O. Keysan and M. Mueller, "Current and future development of the C-Gen lightweight direct drive generator for wave and tidal energy", *European Wave and Tidal Energy Conference*, pp. 352-359, Uppsala, Sweden, 7-10 September 2009
- [4] H. Polinder, D. Bang, R.P.J.O.M. van Rooij, A.S. McDonald, M.A. Mueller, "10 MW wind turbine direct-drive generator design with pitch or active speed stall control", *IEEE Int Electric Machines and Drives Conf.*, Antalya, Turkey, May 2007
- [5] T. Haring, K. Forsman, T. Huhtanen and M. Zawadzki, "Direct drive – opening a new era in many applications", *Pulp and Paper Industry Technical Conference*, pp. 171-179, 16-20 June 2003
- [6] E. Spooner, P. Gordon, J.R. Bumby and C.D. French, "Lightweight ironless-stator PM generators for direct-drive wind turbines", *IEE Proceedings – Electric Power Applications*, vol. 152, pp. 17-26, Jan. 2005
- [7] A. E. Fitzgerald, C. Kingsley (Jr.), S. D. Umans, 2003. *Electrical Machinery*. 6th Ed. New York: McGraw-Hill. pp. 112-129